

## Short communication

Dielectric and mechanical properties of porous  $\text{Si}_3\text{N}_4$  ceramics prepared via low temperature sinteringYongfeng Xia<sup>a,b</sup>, Yu-Ping Zeng<sup>a,\*</sup>, Dongliang Jiang<sup>a</sup><sup>a</sup> Shanghai Institute of Ceramics, Chinese Academy of Sciences, 1295 Dingxi Road, Shanghai 200050 PR China<sup>b</sup> Graduate School of Chinese Academy of Sciences, Beijing 100039, PR China

Received 18 June 2008; received in revised form 30 July 2008; accepted 18 September 2008

Available online 14 October 2008

## Abstract

Borophosphosilicate bonded porous silicon nitride ( $\text{Si}_3\text{N}_4$ ) ceramics were fabricated in air using a conventional ceramic process. The porous  $\text{Si}_3\text{N}_4$  ceramics sintered at 1000–1200 °C shows a relatively high flexural strength and good dielectric properties. The influence of the sintering temperature and contents of additives on the flexural strength and dielectric properties of porous  $\text{Si}_3\text{N}_4$  ceramics were investigated. Porous  $\text{Si}_3\text{N}_4$  ceramics with a porosity of 30–55%, flexural strength of 40–130 MPa, as well as low dielectric constant of 3.5–4.6 were obtained.

© 2008 Elsevier Ltd and Techna Group S.r.l. All rights reserved.

**Keywords:** Porous  $\text{Si}_3\text{N}_4$  ceramics; Dielectric constant; Borophosphosilicate; Low temperature sintering

## 1. Introduction

Radome materials for harsh working conditions demand a series of critical properties, such as low dielectric constant, high mechanical strength, excellent thermal shock resistance and rain erosion resistance [1]. Nowadays, silicon ceramics are mainly used as materials for radome and antenna windows owing to their excellent dielectric properties (dielectric constant  $\sim 3.5$ ) [2]. However, their poor strength (usually less than 80 MPa) [3] and rain erosion resistance are not adequate for high speed vehicles.

Silicon nitride ( $\text{Si}_3\text{N}_4$ ) ceramics have many superior properties, such as high-temperature strength, good oxidation resistance, thermal–chemical corrosion resistance, thermal shock resistance, low thermal expansion coefficient and good dielectric property [4–6]. The dielectric constant ( $\epsilon$ ) of  $\alpha$ - $\text{Si}_3\text{N}_4$  is 5.6 and  $\beta$ - $\text{Si}_3\text{N}_4$  is 7.9 at room temperature, respectively. However, the dielectric constant of  $\text{Si}_3\text{N}_4$  is still high for practical application. Pore design is generally believed as an effective way to decrease the dielectric constant of materials, but pores can also deteriorate the mechanical properties of ceramic materials. Therefore, it is important to keep dielectric and mechanical

properties balanced to meet the practical application. Porous  $\text{Si}_3\text{N}_4$  ceramics can be prepared in different ways, such as, adding fugitive substance [7], freeze drying [8], carbothermal nitridation [9], combustion synthesis [10], *in situ* reaction bonding [1], etc. As a covalent solid,  $\text{Si}_3\text{N}_4$  is difficult to densify without a sintering additive. Usually, metal oxides ( $\text{Y}_2\text{O}_3 + \text{Al}_2\text{O}_3$  [11],  $\text{Er}_2\text{O}_3$  [12],  $\text{Yb}_2\text{O}_3$  [13]) additives are required to get dense  $\text{Si}_3\text{N}_4$  ceramics through liquid-phase sintering. However, the sintering temperature is still high. In order to obtain  $\text{Si}_3\text{N}_4$  ceramics at low temperature, low temperature liquid phases, such as  $\text{SiP}_2\text{O}_7$  [14],  $\text{MgO-Al}_2\text{O}_3\text{-SiO}_2$  system [15],  $\text{SiO}_2$  [16], borophosphosilicate ( $\text{SiO}_2\text{-B}_2\text{O}_3\text{-P}_2\text{O}_5$ ) [17], etc., are used.

In this work, borophosphosilicate glass was used as sintering additive to prepare porous  $\text{Si}_3\text{N}_4$  ceramics. The sintering behavior and the effect of additives on the porosity, flexural strength and dielectric constants of specimens were investigated.

## 2. Experimental procedure

$\alpha$ - $\text{Si}_3\text{N}_4$  (SN-E10, purity > 99.5%,  $\alpha$  ratio > 95%, average particle size 0.5  $\mu\text{m}$ ; UBE Industries, Ltd., Tokyo, Japan),  $\text{H}_3\text{PO}_4$  (purity  $\geq 85$  wt.%; Lingfeng company, Shanghai, China) and  $\text{H}_3\text{BO}_3$  (purity  $\geq 99.5$  wt.%; Sino-pharm Chemical Reagent Co., SCRC; Shanghai, China), Ultra-fine  $\text{SiO}_2$  (30 nm, Jialian Chemical Engineering Co. Ltd., Nanping, China) were used as the starting materials. For the preparation

\* Corresponding author.

E-mail address: [yuping-zeng@mail.sic.ac.cn](mailto:yuping-zeng@mail.sic.ac.cn) (Y.-P. Zeng).

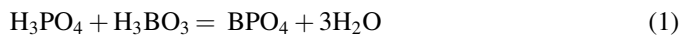
of borophosphosilicate glass, a mixture of  $\text{H}_3\text{PO}_4$ ,  $\text{H}_3\text{BO}_3$  and  $\text{SiO}_2$  in the weight ratio of 1.77:1.38:4 was calcinated at  $500^\circ\text{C}$  with heating and cooling rates of  $2^\circ\text{C}/\text{min}$  with held for 2 h. With regard to the porous  $\text{Si}_3\text{N}_4$  ceramics preparation, a mixture of  $\alpha\text{-Si}_3\text{N}_4$ ,  $\text{H}_3\text{PO}_4$  and  $\text{H}_3\text{BO}_3$  was ball-milled in water for 24 h;  $\text{SiO}_2$  is the oxidation of  $\text{Si}_3\text{N}_4$  during sintering. After being dried and sieved through a 100-mesh ( $154\ \mu\text{m}$ ) screen, the powder was pressed into rectangular bars with dimensions of  $4.5\ \text{mm} \times 10.0\ \text{mm} \times 50.0\ \text{mm}$ , the bars were then cold isostatically pressed at 200 MPa. The bars were firstly heated in air at  $500^\circ\text{C}$  with heating rate of  $2^\circ\text{C}/\text{min}$  and held for 2 h to prevent the pore expansion resulting from the volatilization of  $\text{H}_3\text{PO}_4$  and  $\text{H}_3\text{BO}_3$ , then sintered at  $1000\text{--}1200^\circ\text{C}$  with heating and cooling rates of  $5^\circ\text{C}/\text{min}$  and held for 2 h in air atmosphere.

Differential thermal analysis (DTA) and thermogravimetry (TG) were performed using STA-429 (Netzsch, Germany) differential thermal analyzer with a speed of  $10^\circ\text{C}/\text{min}$  in air. Specimens were machined into a rectangle bar with dimensions of  $3.0\ \text{mm} \times 4.0\ \text{mm} \times 36.0\ \text{mm}$  to measure the flexural strength via the three point bending test (Model AUTOGRAF AG-I, Shimadzu, Japan), the support distance of 30.0 mm and a cross-head speed of 0.5 mm/min were used. The open porosity and bulk density were determined by the Archimedes method using distilled water as medium. Phase analysis was conducted by X-ray diffraction (XRD) via a computer-controlled diffractometer (Model RAX-10, Rigaku, Japan) with Cu  $\text{K}\alpha$  radiation (wavelength of  $1.5418\ \text{\AA}$ ). Morphology of porous  $\text{Si}_3\text{N}_4$  ceramics was observed by scanning electron microscopy (SEM) (Model JXA-8100, JEOL, Tokyo, Japan). The complex permittivities of the specimens with the size of  $\varnothing 20.0\ \text{mm} \times 1.1\ \text{mm}$  were measured in the frequency range of 100 MHz to 1 GHz at room temperature by RF impedance/material analyzer (Model 4291B, Agilent, USA)

### 3. Results and discussion

#### 3.1. Characterization of borophosphosilicate glass

$\text{H}_3\text{PO}_4$  can react with  $\text{H}_3\text{BO}_3$  at  $\sim 100^\circ\text{C}$  as follows [14]:



The crystal structure of  $\text{BPO}_4$  contains  $\text{BO}_4$  and  $\text{PO}_4$  tetrahedron. Meanwhile,  $\text{BPO}_4$  is a copolymer of two water soluble and low melting oxides: boric oxide and phosphorous oxide.  $\text{BPO}_4$  is a chemical inert glass with a good dielectric property ( $\varepsilon \approx 4$ ) [17]. Thus, it is appropriate to use  $\text{BPO}_4$  as the sintering additive in  $\text{Si}_3\text{N}_4$  preparation. Moreover, the strength of  $\text{Si}_3\text{N}_4$  ceramics can be considerably improved by the addition of  $\text{BPO}_4$  [18].

Fig. 1 shows the XRD pattern of the borophosphosilicate glass. The pattern can be indexed to two phases:  $\text{BPO}_4$  and  $\text{B}_2\text{O}_3$ .  $\text{B}_2\text{O}_3$  is derived from excessive  $\text{H}_3\text{BO}_3$ , which is also beneficial for decreasing sintering temperature. Fig. 2 shows the TG/DTA curves for the mixture of  $\text{H}_3\text{PO}_4$ ,  $\text{H}_3\text{BO}_3$  and  $\text{SiO}_2$ . The curves can be divided into two regions. From  $70^\circ\text{C}$  to

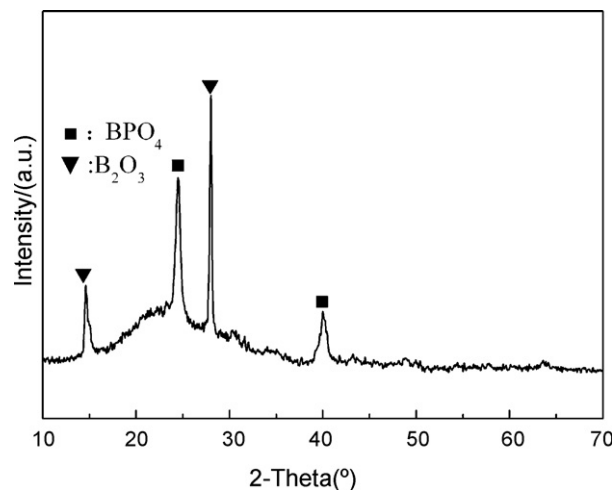


Fig. 1. XRD pattern of borophosphosilicate in the mass ratio of  $\text{H}_3\text{BO}_3/\text{H}_3\text{PO}_4/\text{SiO}_2 = 1.77:1.38:4$  sintered at  $500^\circ\text{C}$  for 2 h.

$180^\circ\text{C}$ , a sharp endothermic peak is observed and the weight loss is about 20 wt.%, corresponding to the formation of  $\text{BPO}_4$  and evaporation of  $\text{H}_2\text{O}$ . Above  $180^\circ\text{C}$ , the obvious weight loss is not observed in the TG, the DTA curve shows a wide peak owing to the crystallization of  $\text{BPO}_4$ , which was also reported by R. Hsu [19].

#### 3.2. Phase and microstructure analysis of porous $\text{Si}_3\text{N}_4$ ceramics

Fig. 3 shows the XRD patterns of  $\text{Si}_3\text{N}_4$  raw powder and porous  $\text{Si}_3\text{N}_4$  ceramics. Compared to the pattern of raw  $\text{Si}_3\text{N}_4$  powder, the weak peaks of  $\text{BPO}_4$  and cristobalite ( $\text{SiO}_2$ ) are found in the sintered  $\text{Si}_3\text{N}_4$  ceramics. The relatively low content of  $\text{BPO}_4$  indicates that the borophosphosilicate glass is amorphous, and the little amount of cristobalite ( $\text{SiO}_2$ ) results from partial oxidation of  $\text{Si}_3\text{N}_4$  in air [20].

Fig. 4 shows the relationship between sintering temperature and porosities of  $\text{Si}_3\text{N}_4$  ceramics. The content of additives has

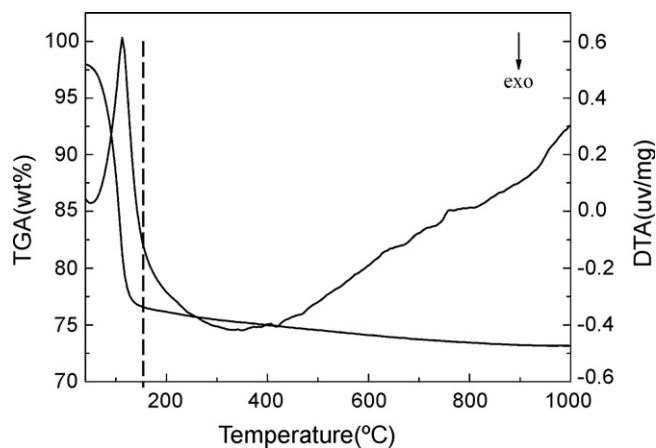


Fig. 2. Thermogravimetry (TG)–differential thermal analysis (DTA) curves of borophosphosilicate in the mass ratio of  $\text{H}_3\text{BO}_3/\text{H}_3\text{PO}_4/\text{SiO}_2 = 1.77:1.38:4$ .

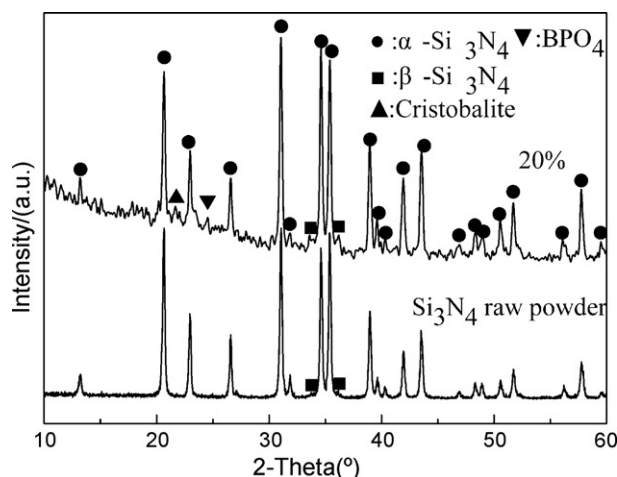


Fig. 3. XRD pattern of  $\text{Si}_3\text{N}_4$  raw powders and  $(\text{H}_3\text{BO}_3 + \text{H}_3\text{PO}_4)$  bonded silicon nitride ( $\text{Si}_3\text{N}_4$ ) ceramic sintered at  $1150^\circ\text{C}$  for 2 h.

great effect on the porosity of porous  $\text{Si}_3\text{N}_4$  ceramics. When the sintering temperature is below  $1000^\circ\text{C}$ , the borophosphosilicate glass is helpful for  $\text{Si}_3\text{N}_4$  densification during sintering process. The porosity of  $\text{Si}_3\text{N}_4$  decreases with the increase in the content of borophosphosilicate glass. When the sintering temperature is above  $1100^\circ\text{C}$ , the samples with more borophosphosilicate glass have higher porosity due to the evaporation of borophosphosilicate glass. On the other hand, with increasing sintering temperature, the porosity decreases first and then increases. For example, the porosity of specimen with 10% additives is 46–32% with the sintering temperature

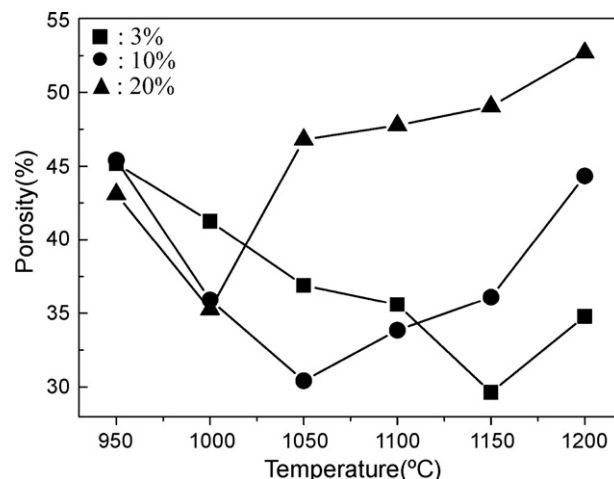


Fig. 4. Relationship between sintering temperature and porosities of  $\text{Si}_3\text{N}_4$  ceramics with different contents of additives.

from  $950^\circ\text{C}$  to  $1050^\circ\text{C}$ , but when the sintering temperature is increased to  $1200^\circ\text{C}$ , the porosity is 43%. This phenomenon is quite consistent with the glass properties, which is in favor of sintering process at low temperature instead of high sintering temperature owing to glass volatilization.

Fig. 5 shows the SEM images of the  $\text{Si}_3\text{N}_4$  ceramics. The SEM micrographs indicate that both glass and sintering temperature have great effects on the microstructure of the porous  $\text{Si}_3\text{N}_4$ . The  $\text{Si}_3\text{N}_4$  sintering processing is very complex, which is related to the glass evaporation,  $\text{Si}_3\text{N}_4$  oxidation and oxidized-derived  $\text{SiO}_2$  reaction with additives. Therefore, the

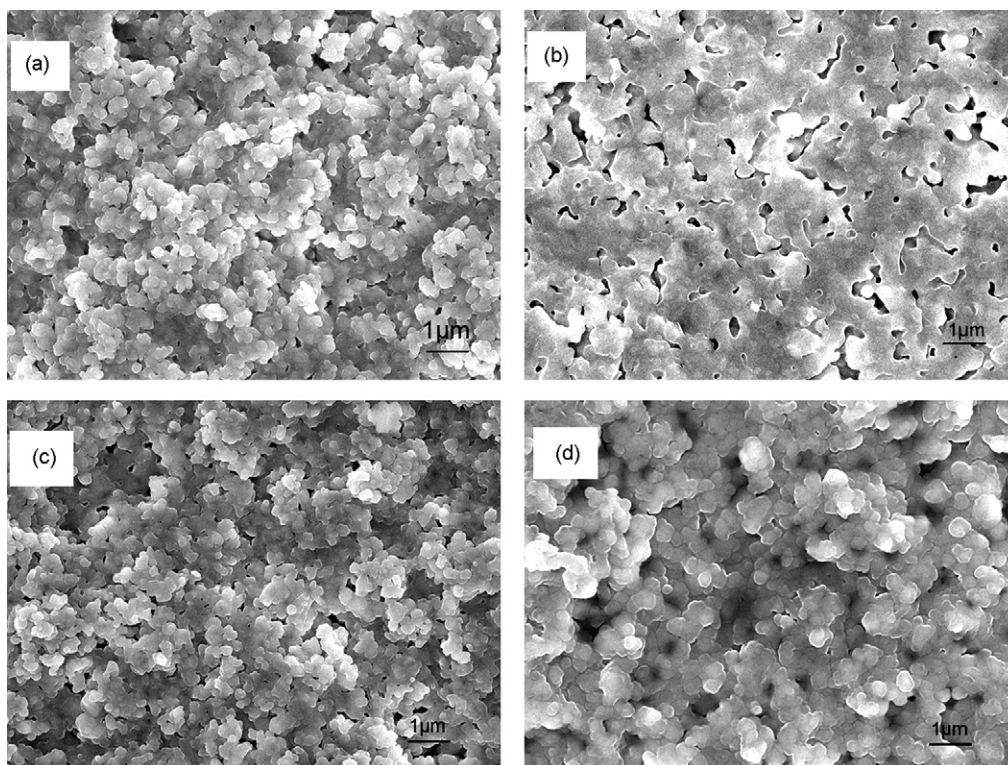


Fig. 5. Microstructure of porous silicon nitride ( $\text{Si}_3\text{N}_4$ ) at different sintering temperatures with different contents of additives: (a)  $1050^\circ\text{C}$ , 3 wt.%; (b)  $1150^\circ\text{C}$ , 3 wt.%; (c)  $1150^\circ\text{C}$ , 10 wt.%; (d)  $1150^\circ\text{C}$ , 20 wt.%.



different sintering temperatures and the different contents of additives result in the different microstructure.

### 3.3. Mechanical and dielectric properties of porous $\text{Si}_3\text{N}_4$ ceramics

Generally, the flexural strength of porous ceramics is mainly dependent on porosity. The strength ( $\sigma$ ) of porous ceramics is expressed as in the following equation [21,22]:

$$\sigma = \sigma_0 \exp(-\beta P) \quad (2)$$

where  $\sigma_0$  is the strength at a porosity of 0,  $\beta$  is the structural factor, and  $P$  is the porosity. Fig. 6 shows the flexural strength of the sintered porous  $\text{Si}_3\text{N}_4$  ceramics. The flexural strength is in the range of 30–130 MPa. The maximal flexural strength is 130 MPa when the sintering temperature is 1150 °C and the content of additive is 3 wt.%. More additives result in the improvement of flexural strength of  $\text{Si}_3\text{N}_4$  at lower sintering temperature. However, more additives lead to decrease in flexural strength at higher temperature because of borophosphosilicate glass volatilization. The flexural strength increases firstly and then decreases, which is consistent with the result of Fig. 4. As shown in Fig. 6(b), the porosity of  $\text{Si}_3\text{N}_4$  dominates the mechanical strength as expected from Eq. (2). Meanwhile,

the flexural strength is affected by cristobalite ( $\text{SiO}_2$ ) oxidized-derived from  $\text{Si}_3\text{N}_4$ . The cristobalite formed in  $\text{Si}_3\text{N}_4$  oxidation is harmful for the strength of specimens, if the volume of cristobalite is larger than 12 vol% of specimen, which will have cracks [23].

According to the mixture rule, the dielectric constant of the two-phase composite is calculated as follows [24]:

$$\varepsilon = V_1 \varepsilon_1 + V_2 \varepsilon_2 \quad (3)$$

where  $\varepsilon$  is the dielectric constant of the composite,  $V_1$  and  $V_2$  are the volume fractions of phase 1 and phase 2, respectively;  $\varepsilon_1$  and  $\varepsilon_2$  are the dielectric constants of the phases. The variation of  $\varepsilon$  with porosity can be considered by using an approximation if the phase 2 is porosity ( $\varepsilon = 1$ ). Eq. (3) reduces to

$$\varepsilon = \varepsilon_0 - P(\varepsilon_0 - 1) \quad (4)$$

where  $\varepsilon_0$  is the dielectric constant of phase 1, and the fractional porosity is  $P$  [25]. It can be seen from Eq. (4) that the dielectric constant of porous ceramic decreases with increase in porosity.

Fig. 7 shows the relationship between the dielectric constant ( $\varepsilon$ ) of the specimens and frequency. The dielectric constant of porous  $\text{Si}_3\text{N}_4$  is influenced by the porosity,  $\text{Si}_3\text{N}_4$ , as well as the second phase, which consists of borophosphosilicate glass and cristobalite. Fig. 7(a) and (b) indicates that for the specimens with 3% additives, the higher sintering temperature results in higher dielectric constants, owing to the porosity having more effects than that of the oxidized-derived cristobalite. It can be seen from Eq. (3) that the constant of composite decreases more when the porosity ( $\varepsilon \approx 1$ ) and the content of cristobalite ( $\varepsilon \approx 3.5$ ) increase in the same magnitude. The dielectric constants of the specimens with 3%, 10%, and 20% additives are also shown in Fig. 7(b)–(d). The dielectric constant does not have great variation with increasing frequency. For 20% additive, namely curve in Fig. 7(d), the increase in porosity and borophosphosilicate glass result in the decrease in dielectric constants. However, the dielectric constant of curve in Fig. 7(c) is higher than that of the curve in Fig. 7(a) although it contains more borophosphosilicate glass, due to lower porosity. So porosity is the dominating factor for the dielectric constant of porous ceramics.

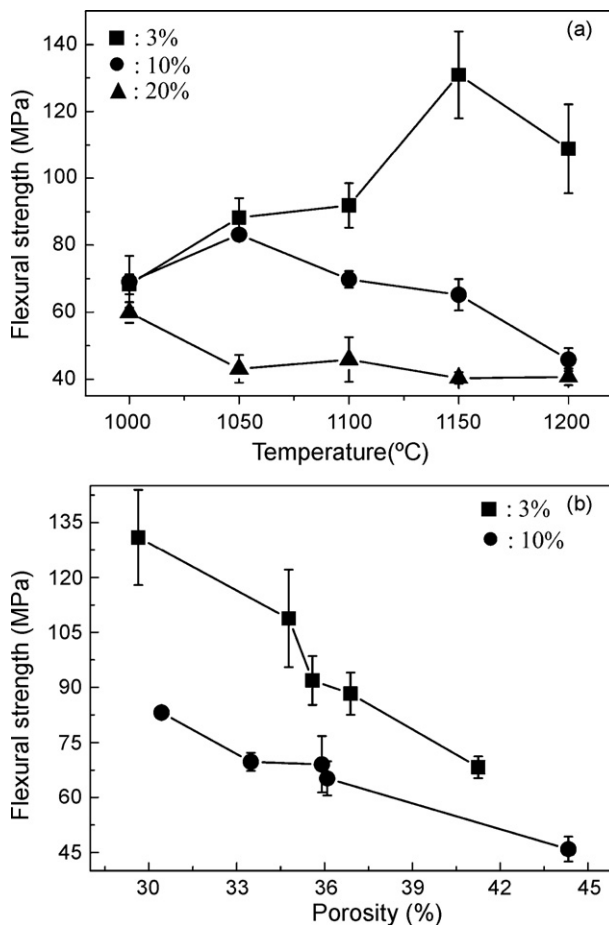


Fig. 6. Flexural strength of porous silicon nitride ceramics ( $\text{Si}_3\text{N}_4$ ) with (a) different contents of additives at different sintering temperatures, (b) different porosities.

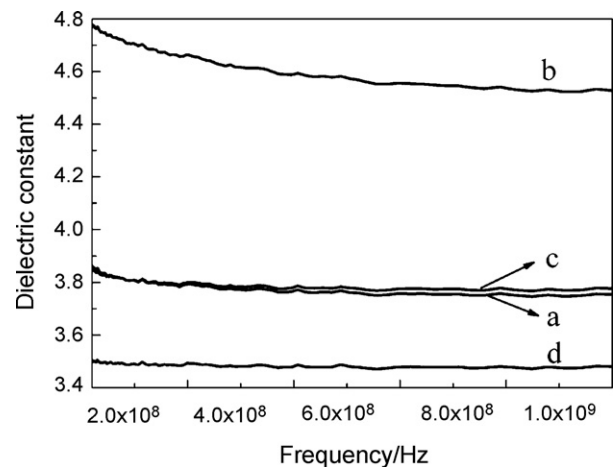


Fig. 7. Dielectric constant ( $\varepsilon$ ) of porous silicon nitride ( $\text{Si}_3\text{N}_4$ ) at different sintering temperatures with different contents of additives: (a) 1000 °C, 3 wt.%; (b) 1100 °C, 3 wt.%; (c) 1100 °C, 10 wt.%; (d) 1100 °C, 20 wt.%.

#### 4. Conclusions

Porous silicon nitride ceramics were fabricated at low temperature in air, using  $\text{H}_3\text{BO}_3$  and  $\text{H}_3\text{PO}_4$  as sintering additives. By changing the contents of additives and sintering temperature, porous  $\text{Si}_3\text{N}_4$  ceramics with flexural strength of 30–130 MPa, porosity of 30–55% and dielectric constants of 3.5–4.6 can be obtained.

#### Acknowledgements

The authors would like to thank the “Plan of Outstanding Talents” of the Chinese Academy of Sciences and the Shanghai of Committee Science and Technology under the object “07jp14093” for the financial support. The comments of the reviewers are greatly appreciated.

#### References

- [1] S.Q. Ding, Y.P. Zeng, D.L. Jiang, Oxidation bonding of porous silicon nitride ceramics with high strength and low dielectric constant, *Mater. Lett.* 61 (11–12) (2006) 2277–2280.
- [2] T.M. Place, D.W. Bridges, Fused quartz reinforced silica composites, in: *Proceedings of the 10th symposium on electro-magnetic windows*, Georgia Institute of Technology, Atlanta, Georgia, USA, 1970, pp. 115–119.
- [3] J.S. Lyons, T.T. Star, Strength and toughness of slip-cast fused-silica composites, *J. Am. Ceram. Soc.* 77 (6) (1994) 1673–1675.
- [4] F.L. Riley, Silicon nitride and related materials, *J. Am. Ceram. Soc.* 83 (2) (2000) 245–265.
- [5] G. Ziegler, J. Heinrich, G. Wotting, Relationships between processing, microstructure and properties of dense and reaction-bonded silicon nitride, *J. Mater. Sci.* 22 (9) (1987) 3041–3086.
- [6] A.J. Pyzik, D.R. Beaman, Microstructure, Properties of self-reinforced silicon nitride, *J. Am. Ceram. Soc.* 76 (11) (1993) 2737–2744.
- [7] D. Aranzazu, H. Stuart, Characterisation of porous silicon nitride materials produced with starch, *J. Eur. Ceram. Soc.* 24 (2) (2004) 413–419.
- [8] T. Fukasawa, Z.Y. Deng, M. Ando, Synthesis of porous silicon nitride with unidirectionally aligned channels using freeze-drying process, *J. Am. Ceram. Soc.* 85 (9) (2002) 2151–2155.
- [9] S.Y. Shan, J.F. Yang, J.Q. Gao, W.H. Zhang, Z.H. Jin, Porous silicon nitride ceramics prepared by reduction–nitridation of silica, *J. Am. Ceram. Soc.* 88 (9) (2005) 2594–2596.
- [10] D.Y. Chen, B.L. Zhang, H.R. Zhuang, W.L. Li, Combustion synthesis of network silicon nitride porous ceramics, *Ceram. Int.* 29 (4) (2003) 363–364.
- [11] J.F. Yang, T. Ohji, Influence of yttria-alumina content on sintering behavior and microstructure of silicon nitride ceramics, *J. Am. Ceram. Soc.* 83 (8) (2000) 2094–2096.
- [12] C. Kaval, Effect of grain size distribution on the strength of porous  $\text{Si}_3\text{N}_4$  ceramics composed of elongated  $\beta$ - $\text{Si}_3\text{N}_4$  grains, *J. Mater. Sci.* 36 (23) (2001) 5713–5717.
- [13] J.F. Yang, Z.Y. Deng, T. Ohji, Fabrication and characterization of porous silicon nitride ceramics using  $\text{Yb}_2\text{O}_3$  as sintering additive, *J. Eur. Ceram. Soc.* 23 (2) (2003) 371–378.
- [14] F. Chen, Q. Shen, F.Q. Yan, L.M. Zhang, Pressureless sintering of  $\alpha$ - $\text{Si}_3\text{N}_4$  porous ceramics using a  $\text{H}_3\text{PO}_4$  pore-forming agent, *J. Am. Ceram. Soc.* 90 (8) (2007) 2379–2383.
- [15] J.Q. Li, F. Luo, D.M. Zhu, W.C. Zhou, Influence of phase formation on dielectric properties of  $\text{Si}_3\text{N}_4$  ceramics, *J. Am. Ceram. Soc.* 90 (6) (2007) 1950–1952.
- [16] G.J. Qi, C.R. Zhang, H.F. Hu, F. Cao, S.Q. Wang, Y.G. Jiang, B. Lin, Crystallization behavior of three-dimensional silica fiber reinforced silicon nitride composite, *J. Cryst. Growth* 284 (2) (2005) 293–296.
- [17] B. Li, Z.X. Yue, J. Zhou, Z.L. Gui, L.T. Li, Low dielectric constant borophosphosilicate glass-ceramics derived from sol-gel process, *Mater. Lett.* 54 (1) (2002) 25–29.
- [18] A. Baykal, M. Kizilyalli, M. Toprak, R. Kniep, Hydrothermal and microwave synthesis of boron phosphate,  $\text{BPO}_4$ , *Turk. J. Chem.* 25 (4) (2001) 425–432.
- [19] R. Hsu, P.N. Kumta, T.P. Feist, Modified oxide sol-gel (MOSG) synthesis of borophosphosilicate glasses and glass-ceramics, *J. Mater. Sci.* 30 (12) (1995) 3123–3129.
- [20] U.J. Linus, T. Ogbuji, R. Scott, Bryan, The  $\text{SiO}_2$ - $\text{Si}_3\text{N}_4$  interface, part I: nature of the interface, *J. Am. Ceram. Soc.* 78 (5) (1995) 1272–1278.
- [21] R.L. Coble, W.D. Kingery, Effect of porosity on physical properties of sintered alumina, *J. Am. Ceram. Soc.* 39 (11) (1956) 377–385.
- [22] R.M. Spriggs, Expression for effect of porosity on elastic modulus of polycrystalline refractory materials, particularly aluminum oxide, *J. Am. Ceram. Soc.* 44 (12) (1961) 628–629.
- [23] F.P. Meyer, Fused quartz reinforced silica composites, in: *Proceedings the 15th Symposium on Electromagnetic Windows*, Georgia Institute of Technology, Atlanta, Georgia, 1980, pp. 170–178.
- [24] W.D. Kingery, H.K. Bowen, D.R. Uhlmann, *Introduction to Ceramics*, 2nd ed., Wiley, New York, 1967.
- [25] S.J. Penn, N.M. Alford, A. Templeton, Effect of porosity and grain size on the microwave dielectric properties of sintered alumina, *J. Am. Ceram. Soc.* 80 (7) (1997) 1885–1888.